Synthesis, Characterization, and Theoretical Studies on Heterobinuclear (*p*-cymene)Os(μ-pz)$_2$M (M = Ir, Rh; Hpz = Pyrazole) Complexes

Daniel Carmona,* Joaquina Ferrer, José M. Arilla, Josefa Reyes, Fernando J. Lahoz, Sergio Elipe, F. Javier Modrego, and Luis A. Oro*

Departamento de Química Inorgánica, Instituto de Ciencia de Materiales de Aragón, Universidad de Zaragoza-Consejo Superior de Investigaciones Científicas, 50009 Zaragoza, Spain

Received August 4, 1999

The cationic compounds [(η^6-*p*-cymene)OsCl(Hpz)$_2$]A (A = Cl (**1**), BF$_4$ (**2**)) have been prepared by treating the dimeric [{(η^6-*p*-cymene)OsCl}$_2$(μ-Cl)$_2$] with pyrazole (*p*-cymene = *p*-isopropylmethylbenzene, Hpz = pyrazole). Compounds **1** and **2** are precursors to new heterobinuclear complexes of stoichiometry [(η^6-*p*-cymene)OsCl(μ-pz)$_2$M(COD)] (M = Ir (**3**), Rh (**4**); COD = 1,5-cyclooctadiene). Carbonylation of **3** and **4** produces the dicarbonyls [(η^6-*p*-cymene)OsCl(μ-pz)$_2$M(CO)$_2$] (M = Ir (**5a**), Rh (**6**)) or, in the presence of NaBPh$_4$, the cationic tricarbonyls [(η^6-*p*-cymene)Os(CO)(μ-pz)$_2$M(CO)$_2$]BPh$_4$ (M = Ir (**7**), Rh (**8**)). Complex **5a** in methanol isomerizes to the metal−metal-bonded compound [(η^6-*p*-cymene)Os(μ-pz)$_2$IrCl(CO)$_2$] (**5b**) (first-order kinetics in **5a**; $k_{obs} = 3.8 \times 10^{-4}$ s^{-1} (room temperature), $\Delta H^{\ddagger} = 93$ kJ mol^{-1}, $\Delta S^{\ddagger} = 7$ J K^{-1} mol^{-1}). The molecular structures of [(η^6-*p*-cymene)OsCl(μ-pz)$_2$Rh(CO)$_2$] (**6**) and [(η^6-*p*-cymene)Os(CO)(μ-pz)$_2$Rh(CO)$_2$]BPh$_4$ (**8**) have been determined by X-ray diffraction methods. In both cases, the molecules contain (η^6-*p*-cymene)Os and Rh(CO)$_2$ moieties bridged by two pyrazolate groups. The osmium−rhodium distances, 3.6231(5) Å (**6**) or 3.7012(6) Å (**8**), exclude any direct intermetallic interaction. The metal−metal-bonded halide carbonyl complexes [(η^6-*p*-cymene)Os(μ-pz)$_2$Ir(CO)$_2$] (X = Br (**9**), I (**10**)) and [(η^6-*p*-cymene)Os(μ-pz)$_2$RhI(CO)] (**12**), as well as the OsRh compound [(η^6-*p*-cymene)OsBr(μ-pz)$_2$Rh(CO)$_2$] (**11**), have been prepared by metathetical reaction on the corresponding dicarbonyls **5a**,**b** and **6** with sodium halides. The molecular structures of **10** and **12** have been elucidated by diffractometric means. The metal−metal distances, 2.7196(6) Å (Os−Ir, **10**) and 2.6936(9) Å (Os−Rh, **12**), confirm the presence of metal−metal bonds. In the solid state, complex **12** crystallizes as a dimer of two dinuclear moieties through an asymmetric diiodide bridge. A theoretical study of the related RuIr dicarbonyl chloride isomers [(η^6-*p*-cymene)RuCl(μ-pz)$_2$Ir(CO)$_2$] (**13a**) and [(η^6-*p*-cymene)Ru(μ-pz)$_2$IrCl(CO)$_2$] (**13b**) is also reported.

Introduction

In the field of organometallic chemistry the area of bimetallic complexes bonded to flexible and firmly binucleating anionic ligands has aroused increased interest. Of particular interest are the very versatile pyrazolate ligands, which can straddle an unusually wide range of intermetallic separations to hold two adjacent metal centers in chemically stable configurations.[1]

While an extensive chemistry on homobinuclear rhodium,[2] iridium,[3] and ruthenium[4] complexes with pyrazolate bridging ligands has been thoroughly investigated, heterobinuclear complexes containing platinum-group metals have been scarcely studied.[5]

In this context, we have previously reported a series of heterobinuclear RuM dicarbonyl complexes of stoichiometry [RuM(*p*-cymene)X(Pz)$_2$(CO)$_2$] (M = Rh, Ir; *p*-cymene = *p*-isopropylmethylbenzene; X = Cl, Br, I; Pz = pyrazolate (pz), 3-substituted pyrazolate).[5f,6] The RuIr chloride compounds were isolated as mixtures of two isomers whose separation was achieved only in some instances. The complexes were independently

(1) (a) Trofimenko, S. *Prog. Inorg. Chem.* **1986**, *34*, 115. (b) Oro, L. A.; Carmona, D.; Esteban, M. *Trends Organomet. Chem.* **1994**, *1*, 565. (c) La Monica, G.; Ardizzoia, G. A. *Prog. Inorg. Chem.* **1997**, *46*, 151.

(2) (a) Usón, R.; Oro, L. A.; Ciriano, M. A.; Pinillos, M. T.; Tiripicchio, A.; Tiripicchio-Camellini, M. *J. Organomet. Chem.* **1981**, *205*, 247. (b) Usón, R.; Oro, L. A.; Ciriano, M. A.; Carmona, D.; Tiripicchio, A.; Tiripicchio-Camellini, M. *J. Organomet. Chem.* **1982**, *224*, 69. (c) Oro, L. A.; Carmona, D.; Lamata, M. P.; Apreda, M. C.; Foces-Foces, C.; Cano, F. H.; Maitlis, P. M. *J. Chem. Soc., Dalton Trans.* **1984**, 1823. (d) Elguero, J.; Esteban, M.; Grenier-Loustalot, M. F.; Oro, L. A.; Pinillos, M. T. *J. Chim. Phys.* **1984**, *81*, 251. (e) Oro, L. A.; Carmona, D.; Lamata, M. P.; Foces-Foces, C.; Cano, F. H. *Inorg. Chim. Acta* **1985**, *97*, 19. (f) Oro, L. A.; Carmona, D.; Pérez, P. L.; Esteban, M.; Tiripicchio, A.; Tiripicchio-Camellini, M. *J. Chem. Soc., Dalton Trans.* **1985**, 973. (g) Carmona, D.; Oro, L. A.; Pérez, P. L.; Tiripicchio, A.; Tiripicchio-Camellini, M. *J. Chem. Soc., Dalton Trans.* **1989**, 1427. (h) Carmona, D.; Lamata, M. P.; Esteban, M.; Lahoz, F. J.; Oro, L. A.; Apreda, M. C.; Foces-Foces, C.; Cano, F. H. *J. Chem. Soc., Dalton Trans.* **1994**, 159. (i) Tejel, C.; Villoro, J. M.; Ciriano, M. A.; López, J. A.; Eguizábal, E.; Lahoz, F. J.; Bakhmutov, W. I.; Oro, L. A. *Organometallics* **1996**, *15*, 2967.

10.1021/om990624h CCC: $19.00
Publication on Web 02/04/2000

Scheme 1. Solution Equilibrium for the RuIr Complexes [(η^6-*p*-cymene)RuCl(μ-Pz)$_2$Ir(CO)$_2$] and [(η^6-*p*-cymene)Os(μ-Pz)$_2$IrCl(CO)$_2$]

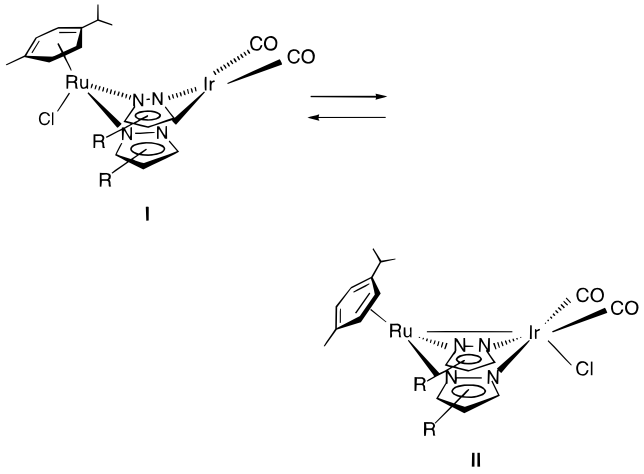

characterized, and the molecular structures, determined by diffractometric methods[6a] for the unsubstituted pyrazolate derivatives [(η^6-*p*-cymene)RuCl(μ-pz)$_2$Ir(CO)$_2$] and [(η^6-*p*-cymene)Ru(μ-pz)$_2$IrCl(CO)$_2$], are schematically represented as I and II, respectively, in Scheme 1. Interestingly, an equilibrium of the two isomers I and II, which implies the migration of the chloride ligand between the metals accompanied by the reversible cleavage and formation of a Ru−Ir bond, is reached in solution. This kind of isomerization, which takes place under mild conditions, is very unusual.[7] In fact, only structures of the type II have been detected for the bromide and iodide analogues [(η^6-*p*-cymene)-Ru(μ-pz)$_2$IrX(CO)$_2$] and, in contrast, only the nonmetal−metal-bonded isomer was observed for the RuRh chloride compounds [(η^6-*p*-cymene)RuCl(μ-Pz)$_2$Rh(CO)$_2$]. Furthermore, the related C_5Me_5 dicarbonyl derivatives [(η^5-C_5Me_5)MX(μ-pz)$_2$M′(CO)$_2$] (M, M′ = Rh, Ir; X = Cl, I, N_3) only adopt nonbonded structures of the type I.[5f,8] The RuIr bromide or iodide, the RuRh chlorides, nor the C_5Me_5 related compounds undergo the aforementioned isomerization process, even under more forcing conditions (reflux in toluene). To shed some light on this peculiar isomerization process, we extended our investigations to include related (*p*-cymene)Os complexes and carried out a theoretical study in an attempt to establish the influence of the M′ metal and halogen on the relative stabilities of structures I and II**.** The results of our study are described in this paper.

Results and Discussion

Heterobimetallic OsIr and OsRh Complexes. (a) Mononuclear (*p*-cymene)Os Precursors. The cationic chloride [(η^6-*p*-cymene)OsCl(Hpz)$_2$]Cl (**1**) can be quantitatively prepared by treating methanolic suspensions of the dimer[9] [{(η^6-*p*-cymene)OsCl}$_2$(μ-Cl)$_2$] with 4 equiv of Hpz (eq 1). The addition of 2 equiv of pyrazole

$$[\{(\eta^6\text{-}p\text{-cymene})\mathrm{OsCl}\}_2(\mu\text{-}\mathrm{Cl})_2] + 4\mathrm{Hpz} \rightarrow 2[(\eta^6\text{-}p\text{-cymene})\mathrm{OsCl(Hpz)_2}]\mathrm{Cl} \quad (1)$$
$$\mathbf{1}$$

to a dichloromethane solution of [{(η^6-*p*-cymene)OsCl}$_2$-(μ-Cl)$_2$] led to a mixture of neutral[10] [(η^6-*p*-cymene)-$OsCl_2$(Hpz)] and **1** in a ca. 5.5:1 ratio, along with unreacted starting material. The formation of cationic **1** could not be avoided, even by use of less than 2 equiv of Hpz. However, the related ruthenium[5a,b,6b] ([(η^6-*p*-cymene)$RuCl_2$(HPz)]) and rhodium or iridium[3c] ([(η^5-C_5Me_5)MCl_2(HPz)]) neutral compounds can be isolated in good yield by starting from the corresponding dimers and using the procedure described above. Noncoordinating anions such as BF_4 can metathetically replace the ionic chloride in **1** to give [(η^6-*p*-cymene)OsCl(Hpz)$_2$]-BF_4 (**2**). Complexes **1** and **2** were characterized on the basis of elemental analysis and NMR and IR spectroscopy (see Experimental Section). The IR spectra in Nujol mulls exhibit an intense[11] ν(NH) band at 3321 cm^{-1} along with a very broad, medium-intensity ν(NH) absorption in the 2500−3200 cm^{-1} region, which suggests that a strong hydrogen bond is present in the solid

(3) (a) Oro, L. A.; Pinillos, M. T.; Royo, M.; Pastor, E. *J. Chem. Res., Synop.* **1984**, 206. (b) Oro, L. A.; Carmona, D.; Puebla, M. P.; Lamata, M. P.; Foces-Foces, C.; Cano, F. H. *Inorg. Chim. Acta* **1986**, *112*, L11. (c) Carmona, D.; Oro, L. A.; Lamata, M. P.; Puebla, M. P.; Ruiz, J.; Maitlis, P. M. *J. Chem. Soc., Dalton Trans.* **1987**, 639. (d) Sola, E.; Bakhmutov, W. I.; Torres, F.; Elduque, A.; López, J. A.; Lahoz, F. J.; Werner, H.; Oro, L. A. *Organometallics* **1998**, *17*, 683. (e) Beveridge, K. A.; Bushnell, G. W.; Stobart, S. R.; Atwood, J. L.; Zaworotko, M. J. *Organometallics* **1983**, *2*, 1447. (f) Atwood, J. L.; Beveridge, K. A.; Bushnell, G. W.; Dixon, K. R.; Eadie, D. T.; Stobart, S. R.; Zaworotko, M. J. *Inorg. Chem.* **1984**, *23*, 4050. (g) Bushnell, G. W.; Fjeldsted, D. O.; Stobart, S. R.; Zaworotko, M. J.; Knox, S. A. R.; Macpherson, K. A. *Organometallics* **1985**, *4*, 1107. (h) Bushnell, G. W.; Decker, M. J.; Eadie, D. T.; Stobart, S. R.; Vefghi, R.; Atwood, J. L.; Zaworotko, M. J. *Organometallics* **1985**, *4*, 2106. (i) Bailey, J. A.; Grundy, S. L.; Stobart, S. R. *Inorg. Chim. Acta* **1996**, *243*, 47. (j) Arthurs, M. A.; Bickerton, J.; Stobart, S. R.; Wang, J. *Organometallics* **1998**, *17*, 2743.

(4) (a) Oro, L. A.; García, M. P.; Carmona, D.; Foces-Foces, C.; Cano, F. H. *Inorg. Chim. Acta* **1985**, *96*, L21. (b) Cabeza, J. A.; Landazuri, C.; Oro, L. A.; Tiripicchio, A.; Tiripicchio-Camellini, M. *J. Organomet. Chem.* **1987**, *322*, C16. (c) Cabeza, J. A.; Landazuri, C.; Oro, L. A.; Belletti, D.; Tiripicchio, A.; Tiripicchio-Camellini, M. *J. Chem. Soc., Dalton Trans.* **1989**, 1093. (d) Carmona, D.; Mendoza, A.; Ferrer, J.; Lahoz, F. J.; Oro, L. A. *J. Organomet. Chem.* **1992**, *431*, 87.

(5) (a) Oro, L. A.; Carmona, D.; García, M. P.; Lahoz, F. J.; Reyes, J.; Cano, F. H.; Foces-Foces, C. *J. Organomet. Chem.* **1985**, *296*, C43. (b) García, M. P.; Portilla, A.; Oro, L. A.; Foces-Foces, C.; Cano, F. H. *J. Organomet. Chem.* **1987**, *322*, 111. (c) Cano, F. H.; Foces-Foces, C.; Oro, L. A.; Pinillos, M. T.; Tejel, C. *Inorg. Chim. Acta* **1987**, *128*, 75. (d) García, M. P.; López, A. M.; Esteruelas, M. A.; Lahoz, F. J.; Oro, L. A. *J. Organomet. Chem.* **1990**, *388*, 365. (e) García, M. P.; López, A. M.; Esteruelas, M. A.; Lahoz, F. J.; Oro, L. A. *J. Chem. Soc., Dalton Trans.* **1990**, 3465. (f) Carmona, D.; Ferrer, J.; Lahoz, F. J.; Oro, L. A.; Reyes, J.; Esteban, M. *J. Chem. Soc., Dalton Trans.* **1991**, 2811. (g) Carmona, D.; Lamata, M. P.; Ferrer, J.; Modrego, J.; Perales, M.; Lahoz, F. J.; Atencio, R.; Oro, L. A. *J. Chem. Soc., Chem. Commun.* **1994**, 575.

(6) (a) Carmona, D.; Ferrer, J.; Mendoza, A.; Lahoz, F. J.; Reyes, J.; Oro, L. A. *Angew. Chem., Int. Ed. Engl.* **1991**, *30*, 1171. (b) Carmona, D.; Ferrer, J.; Oro, L. A.; Trofimenko, S. *Gazz. Chim. Ital.* **1994**, *124*, 35.

(7) (a) Jones, R. A.; Wright, T. C.; Atwood, J. L.; Hunter, W. E. *Organometallics* **1983**, *2*, 470. (b) Bender, R.; Braunstein, P.; Tiripicchio, A.; Tiripicchio-Camellini, M. *Angew. Chem., Int., Ed. Engl.* **1985**, *24*, 861. (c) Braunstein, P.; De Meric de Bellefon, C.; Bouaoud, S.-E.; Grandjean, D.; Halet, J.-F.; Saillard, J.-Y. *J. Am. Chem. Soc.* **1991**, *113*, 5282. (d) Bender, R.; Braunstein, P.; Dedieu, A.; Ellis, P. D.; Huggins, B.; Harvey, E.; Sappa, E.; Tiripicchio, A. *Inorg. Chem.* **1996**, *35*, 1223.

(8) Oro, L. A.; Carmona, D.; Reyes, J.; Foces-Foces, C.; Cano, F. H. *J. Chem. Soc., Dalton Trans.* **1986**, 31.

(9) Cabeza, J. A.; Maitlis, P. M. *J. Chem. Soc., Dalton Trans.* **1985**, 573.

(10) [(η^6-*p*-cymene)$OsCl_2$(Hpz)] was characterized by ^{1}H NMR in $CDCl_3$: δ 12.14 (bs, 1H, NH); 7.80 (bs, 1H, Hpz); 7.50 (bs, 1H, Hpz); 6.36 (bd, 1H, ^3J(HH) = 2.2 Hz, Hpz); 5.90, 5.72 (AA′BB′ system, J(AB) = J(A′B′) = 5.6 Hz, C_6H_4); 2.76 (sp, 1H, C*H*Me_2); 2.24 (s, 3H, Me); 1.21 (d, 6H, ^3J(HH) = 6.9 Hz, CH*Me*$_2$).

(11) Jones, C. J.; McCleverty, J. A.; Rothin, A. S. *J. Chem. Soc., Dalton Trans.* **1986,** 109.

state.[12] The band due to the ν(OsCl)[9,13] vibration was observed at ca. 300 cm^{-1}. The presence of the uncoordinated BF_4 anion in complex **2** is revealed by two strong absorptions[14] centered at ca. 1100 and 520 cm^{-1}.

The ^1H NMR spectrum of **2** is consistent with the presence of two coordinated Hpz ligands per cation. Their chemical shifts and coupling constants are comparable to those previously reported for the homologous ruthenium complex[15] [(η^6-*p*-cymene)RuCl(Hpz)$_2$]BF_4. All the ^1H NMR data of the chloride compound **1** are also comparable to those of the tetrafluoroborate **2**, apart from those for the NH protons. These protons are more deshielded than those of **2** (a difference in chemical shift of 2.4 ppm), and more interestingly, their couplings with the pyrazolate protons H_3, H_4, and H_5 can be directly measured in the spectrum, their values being 2.1, 2.1, and 1.8 Hz, respectively. These results suggest that the strong hydrogen bond N−H···Cl detected by IR spectroscopy in the solid state is also present in chloroform solution. Although a similar behavior has been found in complexes with one diazole ligand,[15,16] in compounds with two diazoles[15] couplings involving the NH protons are rarely observed in solution because they are implicated in rapid prototropism.

(b) Binuclear OsM Diolefin Complexes. Treatment of [(η^6-*p*-cymene)OsCl(Hpz)$_2$]BF_4 (**2**) with the dimers [M(μ-OMe)(COD)]$_2$ (M = Ir, Rh)[17] in the presence of 1 equiv of KOH led to the neutral dinuclear compounds [(η^6-*p*-cymene)OsCl(μ-pz)$_2$M(COD)] (M = Ir (**3**), Rh (**4**)) in ca. 60% (**3**) and 90% (**4**) yields, respectively.

$$[(\eta^6\text{-}p\text{-cymene})\mathrm{OsCl(Hpz)_2}]\mathrm{BF_4} + {}^1/_2[\mathrm{M}(\mu\text{-OMe})(\mathrm{COD})]_2 + \mathrm{KOH} \rightarrow [(\eta^6\text{-}p\text{-cymene})\mathrm{OsCl}(\mu\text{-pz})_2\mathrm{M(COD)}] + \mathrm{MeOH} + \mathrm{KBF_4} + \mathrm{H_2O} \quad (2)$$

M = Ir (**3**), Rh (**4**)

Complexes **3** and **4** were characterized by elemental analysis and IR and ^1H NMR spectroscopy (see Experimental Section). The IR spectra do not show the characteristic NH, BF_4, and C−O vibrations of the starting materials and do show one absorption at 1059 cm^{-1}, which can be assigned to the δ(CH) vibration of the pyrazolate ligand.[18] The ν(OsCl) stretching frequency appears at 304 (**3**) and 302 (**4**) cm^{-1}, as expected for a terminal Os−Cl bond. The ^1H NMR spectra are consistent with the proposed formulation (Chart 1), and they show the inequivalence of the H_3 and H_5 pyrazolate protons and the presence of the *p*-cymene, pz, and COD ligands in the required proportions. The two pyrazolate groups are acting as exobidentate bridging ligands, a situation that has also been found in the crystal structures of the related carbonyl derivatives (see below).

Chart 1. Proposed Structure for Complexes 3 and 4

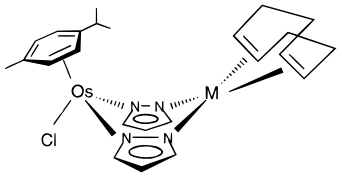

M = Ir (**3**), Rh (**4**)

The preparation of the OsIr compound **3** was accompanied by the formation of the diiridium dimer[19] [Ir(μ-pz)(COD)]$_2$ and the triply bridged diosmium compound[20] [{(η^6-*p*-cymene)Os}$_2$(μ-Cl)(μ-pz)$_2$]BF_4, which accounts for the moderate preparative yield. Scheme 2 illustrates a possible reaction path for the preparation of these compounds. The reaction could proceed through the common undetected intermediate A, formed by abstraction of one of the NH protons on **2** by a methoxo group of the iridium dimer. The cleavage of the Os−N bond in A affords "[Os(*p*-cymene)Cl(Hpz)]$^+$" and "Ir(pz)(COD)" moieties. Reaction of the former with KOH and subsequent dimerization with dissociation of one chloride anion leads to the diosmium cation [{(η^6-*p*-cymene)Os}$_2$(μ-Cl)(μ-pz)$_2$]$^+$. The highly unsaturated "Ir(pz)(COD)" unit dimerizes to the observed product [Ir(μ-pz)(COD)]$_2$. Alternatively, the intermediate A could directly react with KOH, thus removing the remaining NH proton and affording **3**. Comparable redistribution reactions have been reported for binuclear RuRh and RuIr derivatives with two pyrazolate bridging groups.[5f,21]

(c) Binuclear OsM Carbonyl Compounds. When CO is bubbled through dichloromethane solutions of complexes **3** and **4** at room temperature, the dicarbonyl compounds [(η^6-*p*-cymene)OsCl(μ-pz)$_2$M(CO)$_2$] (M = Ir (**5a**), Rh (**6**)) can be isolated in good yield (eq 3).

$$[(\eta^6\text{-}p\text{-cymene})\mathrm{OsCl}(\mu\text{-pz})_2\mathrm{M(COD)}] + 2\mathrm{CO} \rightarrow [(\eta^6\text{-}p\text{-cymene})\mathrm{OsCl}(\mu\text{-pz})_2\mathrm{M(CO)_2}] + \mathrm{COD} \quad (3)$$

M = Ir (**5a**), Rh (**6**)

The IR spectra of complexes **5a** and **6** show two very strong ν(CO) absorptions in the 1996−2081 cm^{-1} region, and these are characteristic of *cis*-dicarbonyl structures.[22] A weak band at ca. 300 cm^{-1} is also observed

(12) Oro, L. A.; Carmona, D.; Lamata, M. P.; Tiripicchio, A.; Lahoz, F. J. *J. Chem. Soc., Dalton Trans.* **1986**, 15, and references therein.
(13) Arthur, T.; Stephenson, T. A. *J. Organomet. Chem.* **1981**, *208*, 369.
(14) Nakamoto, K. *Infrared and Raman Spectra of Inorganic and Coordination Compounds*, 4th ed.; Wiley: New York, 1986; p 132.
(15) Carmona, D.; Ferrer, J.; Oro, L. A.; Apreda, M. C.; Foces-Foces, C.; Cano, F. H.; Elguero, J.; Jimeno, M. L. *J. Chem. Soc., Dalton Trans.* **1990**, 1463.
(16) (a) Elguero, J.; Fruchier, A.; Pardo, M. C. *Org. Magn. Reson.* **1974**, *6*, 272. (b) Claramunt, R. M.; Elguero, J.; Marzin, C.; Seita, J. *An. Quim.* **1979**, *75*, 701. (c) Fruchier, A.; Elguero, J. *Spectrosc. Lett.* **1979**, *12*, 809.
(17) Usón, R.; Oro, L. A.; Cabeza, J. A. *Inorg. Synth.* **1985**, *23*, 126.
(18) Usón, R.; Oro, L. A.; Esteban, M.; Cuadro, A. M.; Navarro, P.; Elguero, J. *Transition Met. Chem.* **1982**, *7*, 234.
(19) (a) Beveridge, K. A.; Bushnell, G. W.; Dixon, D. R.; Eadie, D. T.; Stobart, S. R.; Atwood, J. L.; Zaworotko, M. J. *J. Am. Chem. Soc.* **1982**, *104*, 920. (b) Coleman, A. W.; Eadie, D. T.; Stobart, S. R.; Zaworotko, M. J.; Atwood J. L. *J. Am. Chem. Soc.* **1982**, *104*, 922.
(20) The complex cation [{(η^6-*p*-cymene)Os}$_2$(μ-Cl)(μ-pz)$_2$]$^+$ was spectroscopically detected by ^1H NMR resonance and by mass spectrometry. ^1H NMR ($CDCl_3$, δ): 7.69 (bs, 4H, pz); 6.03 (bs, 2H, pz); 5.81, 5.66 (AA′BB′ system, 8H, J(AB) = J(A′B′) = 5.1 Hz, C_6H_4); 2.64 (sp, 2H, C*H*Me$_2$); 2.32 (s, 6H, Me); 1.10 (d, 12H, ^3J(HH) = 6.8 Hz, CH*Me*$_2$). MS (FAB$^+$): *m*/*z* 819 (M$^+$).
(21) (a) Usón, R.; Oro, L. A.; Ciriano, M. A.; Pinillos, M. T.; Cabeza, J. A. *J. Organomet. Chem.* **1981**, *221*, 249. (b) Usón, R.; Gimeno, J.; Oro, L. A.; Martínez de Ilarduya, J. M.; Cabeza, J. A. *J. Chem. Soc., Dalton Trans.* **1983**, 1729.
(22) (a) Usón, R.; Oro, L. A.; Claver, C.; Garralda, M. A. *J. Organomet. Chem.* **1976**, *105*, 365. (b) Usón, R.; Oro, L. A.; Artigas, J.; Sariego, R. *J. Organomet. Chem.* **1979**, *179*, 65. (c) Bonati, F.; Wilkinson, G. *J. Chem. Soc.* **1964**, *179*, 3156.

Scheme 2. Possible Path for Reaction 2[a]

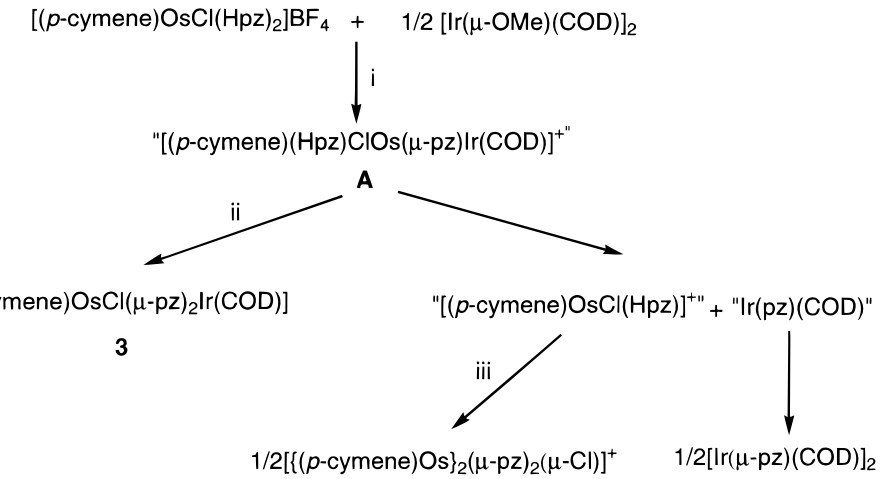

[a] Legend: (i) −MeOH; (ii) +KOH, −H_2O, −KBF_4; (iii) +KOH, −H_2O, −KCl.

and is attributable to a terminal ν(OsCl) vibration. The ^{1}H NMR spectra show the presence in the molecule of the two pyrazolate groups and one *p*-cymene, the signals of which have the expected chemical shifts, multiplicities, and relative intensities (see Experimental Section). The molecular structure of compound **6**, determined by X-ray crystallographic means, agrees with all these spectroscopic data (see below).

As reported for its RuIr homologue[6a] (see Scheme 1), complex **5a** easily isomerizes at room temperature in methanol or chloroform, with a lower rate of isomerization in the latter. The similarity of the NMR data between the RuIr and the OsIr compounds permits us to propose the formulation [(η^6-*p*-cymene)Os(μ-pz)$_2$IrCl(CO)$_2$] (**5b**) for the new OsIr isomer, with the isomerization involving the formal migration of the chloride from the Os to the Ir with concomitant formation of an Os−Ir bond. According to ^{1}H NMR data, the system reached equilibrium in methanol-d_4, at room temperature (K = [**5b**]/[**5a**] = 2.9 ± 0.1). Isomer **5b** is less soluble in methanol than **5a**, and by taking advantage of this property, spectroscopically pure **5b** can be isolated. Thus, pure **5b** slowly separates from methanolic suspensions of **5a**. The progress of the isomerization **5a** → **5b** was monitored by ^{1}H NMR in methanol-d_4. The reaction obeys a first-order rate law in **5a**, and from the value of the rate constant at different temperatures,[23] activation parameters of $\Delta H^{\ddagger}$ = 93 kJ mol^{-1} and $\Delta S^{\ddagger}$ = 7 J K^{-1} mol^{-1} were measured.[24] On the other hand, we have not observed a similar isomerization process for the OsRh analogue [(η^6-*p*-cymene)OsCl(μ-pz)$_2$Rh(CO)$_2$] (**6**) even in refluxing methanol. In summary, the behavior of the OsM systems closely resembles that observed for the RuM analogues.

Bubbling of carbon monoxide through methanolic solutions of compounds **3** and **4** in the presence of $NaBPh_4$ caused, besides the displacement of the coordinated diolefin, the elimination of the terminal chloride ligand and the formation of the cationic tricarbonyls [(η^6-*p*-cymene)Os(CO)(μ-pz)$_2$M(CO)$_2$]BPh_4 (M = Ir (**7**), Rh (**8**)) (eq 4). Alternatively, compound **8** can be prepared by treating methanolic suspensions of compound **6** with CO in the presence of $NaBPh_4$.

$$[(\eta^6\text{-}p\text{-cymene})OsCl(\mu\text{-pz})_2M(COD)] + \underset{M = Ir\ (\mathbf{3}),\ Rh\ (\mathbf{4})}{} 3CO + NaBPh_4 \rightarrow [(\eta^6\text{-}p\text{-cymene})Os(CO)(\mu\text{-pz})_2M(CO)_2]BPh_4 + \underset{M = Ir\ (\mathbf{7}),\ Rh\ (\mathbf{8})}{} COD + NaCl \quad (4)$$

Complexes **7** and **8** were characterized by elemental analysis and IR and ^{1}H NMR spectroscopy (see Experimental Section). Furthermore, the structure of complex **8** was determined by diffractometric methods. The IR spectra show the characteristic bands of the terminal CO groups in the 2000 cm^{-1} region and an absorption at 1581 cm^{-1}, which is assigned to the uncoordinated BPh_4^- anion and reflects the ionic nature of the compounds. The chemical shifts, couplings, and intensities of the resonances in the ^{1}H NMR spectra are in good agreement with a molecular structure containing one *p*-cymene group and two bridging, chemically equivalent pyrazolate ligands, as found in the X-ray molecular structure determination of complex **8**.

(d) Molecular Structures of [(η^6-*p*-cymene)OsCl(μ-pz)$_2$Rh(CO)$_2$] (6) and [(η^6-*p*-cymene)Os(CO)(μ-pz)$_2$Rh(CO)$_2$]BPh_4 (8). Molecular representations of compound **6** and of the cation of complex **8** are shown in Figures 1 and 2, respectively, together with the atom labeling system used. Selected bond distances and angles are listed in Table 1. Both complexes consist of pseudooctahedral osmium(II) and square-planar rhodium(I) atoms connected by two bridging pyrazolate ligands. The resulting OsN_4Rh metallacycles adopt boat conformations; the Cremer and Pople puckering parameters for these complexes are listed in Table 4. The coordination around the osmium atom is completed by one η^6-*p*-cymene ligand and one terminal chloride (**6**) or one terminal CO group (**8**). The rhodium atoms are also bonded, in both cases, to two terminal carbonyl ligands. The Os−Rh distances, 3.6231(5) Å (**6**) and 3.7012(6) Å (**8**), exclude any significant metal−metal interaction. These values correlate with the relative

(23) The k values at 5, 10, 15, and 21 °C were 4.3 × 10^{-5}, 5.9 × 10^{-5}, 1.5 × 10^{-4}, and 3.8 × 10^{-4} s^{-1}, respectively.

(24) Wilkins, R. G. *Kinetics and Mechanism of Reactions of Transition Metal Complexes*, 2nd ed.; VCH: Weinheim, Germany, 1991; p 87.

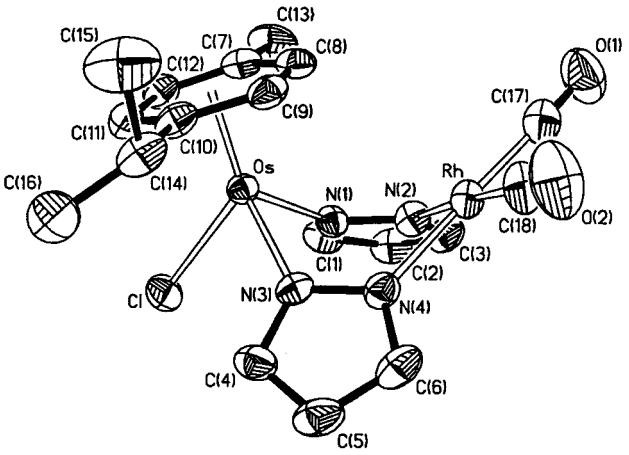

Figure 1. Molecular representation of [(η^6-*p*-cymene)OsCl(μ-pz)$_2$Rh(CO)$_2$] (**6**).

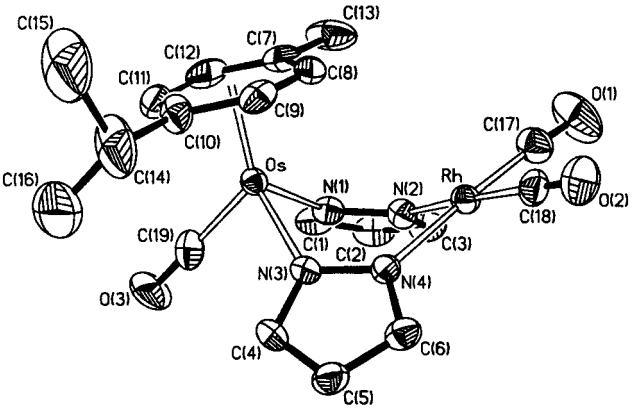

Figure 2. Molecular structure of the cation of the complex [(η^6-*p*-cymene)Os(CO)(μ-pz)$_2$Rh(CO)$_2$]BPh$_4$ (**8**).

folding of the structures observed by the dihedral angles between the two Os−N−N−Rh bridging moieties (β angle) and between the two metal coordination planes (α angle) (see Table 4): longer intermetallic distances imply that both dihedral angles have higher values.[2i]

The Os−N (mean 2.094(4) Å (**6**), 2.074(4) Å (**8**)) and Rh−N (mean 2.070(4) Å (**6**), 2.065(4) Å (**8**)) bond distances compare well with the bond lengths found in the analogous RuRh compound [(η^6-*p*-cymene)RuCl(μ-pz)$_2$Rh(CO)$_2$] (Ru−N mean 2.086(3) Å; Rh−N mean 2.062(4) Å).[6a] The Os−G (G = *p*-cymene centroid) separations are significantly different, with values of 1.668(5) Å in **6** and 1.764(7) Å in **8**. The distance obtained in **6** falls in the range of previously reported Os−*p*-cymene bond distances, 1.63−1.72 Å,[25] in related mono- or polynuclear complexes. However, the value determined in **8** is clearly longer, probably reflecting the lower electron density present on the metal center in this case. In both structures the Os−C(*p*-cymene) distances are significantly different, showing that the *p*-cymene ring is not completely planar but is slightly puckered and adopts, in the case of **6**, a clear boat conformation, with atoms C(7) and C(10) at the bow and stern. The structural parameters of CO and pyrazolate ligands as well as those of the BPh_4 anion are not unusual and do not warrant further comment.

In summary, carbonylation of the chloride diolefin compounds **3** and **4** in polar media, such as methanol, and in the presence of halogen scavangers, such as $NaBPh_4$, afforded the tricarbonyl compounds **7** and **8**, most probably via the dicarbonyl derivatives **5** and **6**, which are the final products in nonpolar media and in the absence of halogen labilizers.

(e) Metathesis with NaX (X = Br, I). Mixtures of the chloride compounds **5a** and **5b**, in methanol, reacted with NaX (X = Br, I), affording the metal−metal-bonded OsIr dicarbonyls [(η^6-*p*-cymene)Os(μ-pz)$_2$IrX(CO)$_2$] (X = Br (**9**), I (**10**)). Under the same conditions, the OsRh complex **6** gave the non-metal−metal-bonded bromide compound [(η^6-*p*-cymene)OsBr(μ-pz)$_2$Rh(CO)$_2$] (**11**) and the metal−metal-bonded iodide monocarbonyl [(η^6-*p*-cymene)Os(μ-pz)$_2$RhI(CO)] (**12**).[26] Complex **12** could be quantitatively prepared by carrying out the reaction in refluxing methanol. However, neither the OsIr compounds **9** and **10** nor the OsRh bromide **11** were converted into the corresponding monocarbonyl complexes in refluxing methanol.

Again, as in the RuM (M = Rh, Ir) chemistry,[5f,6a,b] only for the OsIr-containing derivatives was it possible to detect metal−metal-bonded species. The sole exception was the monocarbonyl OsRh iodide [(η^6-*p*-cymene)-Os(μ-pz)$_2$RhI(CO)] (**12**), in which the elimination of one of the two terminal carbonyls forces the formation of the OsRh bond. Furthermore, from the analogy with the RuM chemistry, neither the bromide nor the iodide metal−metal bonded OsIr derivatives isomerized to the corresponding non-metal−metal-bonded species.

The IR spectra of complexes **9**−**12** show the expected strong ν(CO) absorption bands in the region of 2000 cm^{-1} (see Experimental Section). The ^{1}H NMR data are in good agreement with structures consisting of (*p*-cymene)Os and M(CO)$_2$ (**9**−**11**) or M(CO) (**12**) moieties linked by two exobidentate pyrazolate groups. In particular, the ^{1}H NMR spectral data of the monocarbonyl compound [(η^6-*p*-cymene)Os(μ-pz)$_2$RhI(CO)] (**12**) show the chemical inequivalence of the two bridging pyrazolate ligands. The absence of a symmetry plane relating these two groups renders the osmium center chiral, and accordingly, the *p*-cymene ligand contains two different aromatic AB systems, as well as two diastereotopic methyl isopropyl groups. The characterization of these types of compounds was completed with the X-ray determination of the molecular structures of compounds **10** and **12**.

(f) Molecular Structures of [(η^6-*p*-cymene)Os(μ-pz)$_2$IrI(CO)$_2$] (10) and [(η^6-*p*-cymene)Os(μ-pz)$_2$RhI(CO)] (12). Molecular drawings of complexes **10** and **12** are represented in Figures 3 and 4, respectively. Selected bond distances and angles for **10** and **12** are

(25) (a) Watkins, S. F.; Fronczek, F. R. *Acta Crystallogr., Sect. B* **1982**, *38*, 270. (b) Cabeza, J. A.; Adams, H.; Smith, A. J. *Inorg. Chim. Acta* **1986**, *114*, L17. (c) Michelman, R. I.; Bergman, R. G.; Andersen, R. A. *Organometallics* **1993**, *13*, 2741. (d) Bell, A. G.; Kozminski, W.; Linden, A.; von Philipsborn, W. *Organometallics* **1996**, *15*, 3124. (e) Burrell, A. K.; Steedman, A. J. *Organometallics* **1997**, *16*, 1203

(26) Comparison of the ^{1}H NMR data of the methyls of the *p*-cymene ligand and of the pyrazolate protons of the dicarbonyl compounds **5a**,**b**, **9**, and **11** with those of homologous compounds characterized by diffractometric methods, [(η^6-*p*-cymene)RuCl(μ-pz)$_2$M(CO)$_2$] (M = Rh, Ir), [(η^6-*p*-cymene)Os(μ-pz)$_2$IrCl(CO)$_2$], **6**, and **10**, clearly distinguish between metal−metal-bonded and non-metal−metal-bonded molecules.

Table 1. Selected Bond Distances (Å) and Angles (deg) for the Complexes [(η⁶-*p*-cymene)OsCl(μ-pz)₂Rh(CO)₂] (6) and [(η⁶-*p*-cymene)Os(CO)(μ-pz)₂Rh(CO)₂]BPh₄ (8)

	6 (L = Cl)	**8** (L = CO)		**6** (L = Cl)	**8** (L = CO)
Os−L	2.4129(12)	1.861(7)	Rh−N(2)	2.073(4)	2.062(5)
Os−N(1)	2.091(4)	2.073(4)	Rh−N(4)	2.066(4)	2.068(4)
Os−N(3)	2.097(4)	2.074(4)	Rh−C(17)	1.866(7)	1.856(6)
Os−C(7)	2.217(5)	2.290(6)	Rh−C(18)	1.864(6)	1.871(6)
Os−C(8)	2.177(5)	2.277(7)	C(17)−O(1)	1.142(9)	1.135(7)
Os−C(9)	2.161(4)	2.272(7)	C(18)−O(2)	1.139(8)	1.122(8)
Os−C(10)	2.227(5)	2.263(6)	C(19)−O(3)		1.166(9)
Os−C(11)	2.197(5)	2.199(6)	N(1)−N(2)	1.371(6)	1.362(6)
Os−C(12)	2.195(5)	2.248(6)	N(3)−N(4)	1.370(6)	1.367(6)
L−Os−N(1)	86.02(10)	87.8(2)	N(2)−Rh−N(4)	88.68(16)	89.85(17)
L-Os−N(3)	85.60(11)	90.3(2)	N(2)−Rh−C(17)	91.6(2)	89.5(2)
L−Os−G[a]	127.54(16)	127.0(3)	N(2)−Rh−C(18)	176.1(2)	177.7(2)
N(1)−Os−N(3)	83.81(16)	85.60(17)	N(4)−Rh−C(17)	179.3(2)	176.9(2)
N(1)−Os−G	128.8(2)	126.3(2)	N(4)−Rh−C(18)	88.1(2)	90.6(2)
N(3)−Os−G	129.6(2)	126.9(2)	C(17)−Rh−C(18)	91.6(3)	89.9(3)
Os−C(19)−O(3)		179.7(6)	Rh−C(17)−O(1)	177.4(6)	176.0(6)
			Rh−C(18)−O(2)	176.7(5)	178.4(6)

[a] G represents the centroid of the *p*-cymene ring.

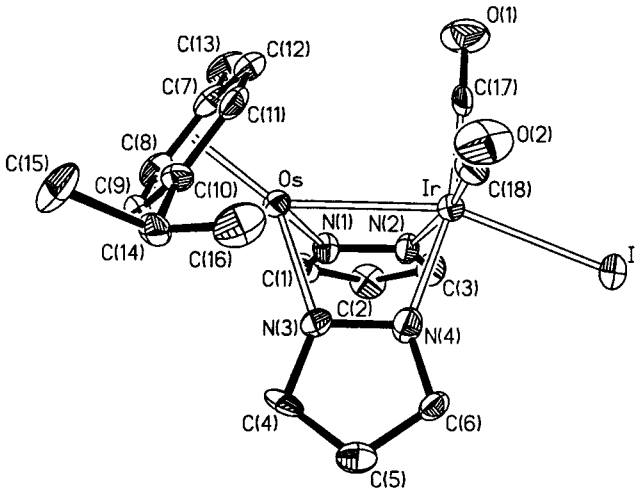

Figure 3. Molecular diagram of [(η⁶-*p*-cymene)Ru(μ-pz)₂IrI(CO)₂] (**10**).

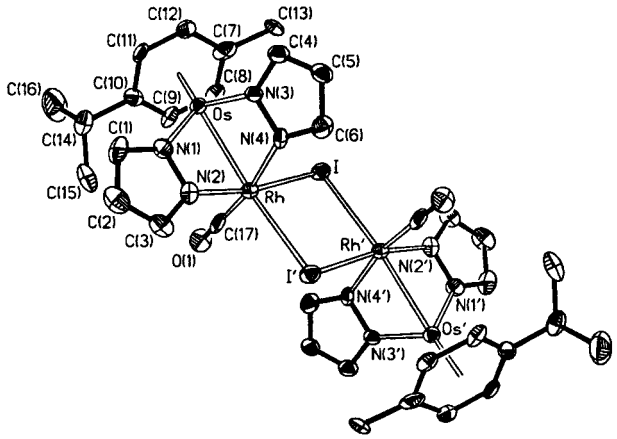

Figure 4. Molecular representation of [(η⁶-*p*-cymene)-Os(μ-pz)₂RhI(CO)] (**12**).

listed in Tables 2 and 3, respectively. Both complexes consist of "(*p*-cymene)Os" and "IrI(CO)₂" (**10**) or "RhI(CO)" (**12**) moieties connected by two bridging pyrazolate ligands and by an Os−M metal−metal bond. It is particularly interesting that great changes are observed in the Os−M separations when these molecular structures are compared with that of the chloride parent compound **6**. Thus, while the osmium and rhodium are separated by 3.6231(5) Å in **6**, the Os−M distances are only 2.7196(6) and 2.6936(9) Å in **10** and **12**, respectively. Compressions of about 1 Å in the Os−M vector account for the formation of metal−metal bonds and reflect the great flexibility of the pyrazolate bridging groups.[1,27] The dihedral angles α and β are consequently smaller (Table 4). The $OsN_4Ir(Rh)$ six-membered rings adopt boat conformations with the metals at the bow and stern. In both complexes, the Os completes its coordination sphere with one η⁶-*p*-cymene ligand separated by normal distances[25] of 1.666(10) and 1.670(9) Å for **10** and **12**, respectively.

Table 2. Selected Bond Distances (Å) and Angles (deg) for the Complex [(η⁶-*p*-cymene)Os(μ-pz)₂IrI(CO)₂] (10)

Os−Ir	2.7196(6)	Ir−I	2.8127(10)
Os−N(1)	2.085(8)	Ir−N(2)	2.070(8)
Os−N(3)	2.056(9)	Ir−N(4)	2.034(8)
Os−C(7)	2.204(11)	Ir−C(17)	1.842(12)
Os−C(8)	2.178(9)	Ir−C(18)	1.859(11)
Os−C(9)	2.182(11)	C(17)−O(1)	1.149(15)
Os−C(10)	2.212(11)	C(18)−O(2)	1.130(13)
Os−C(11)	2.180(10)	N(1)−N(2)	1.357(11)
Os−C(12)	2.172(11)	N(3)−N(4)	1.392(12)
Ir−Os−N(1)	69.8(2)	I−Ir−N(2)	93.0(2)
Ir−Os−N(3)	70.2(2)	I−Ir−N(4)	92.4(2)
Ir−Os−G[a]	140.4(3)	I−Ir−C(17)	100.6(3)
N(1)−Os−N(3)	83.3(3)	I−Ir−C(18)	97.1(4)
N(1)−Os−G	132.8(4)	N(2)−Ir−N(4)	85.2(3)
N(3)−Os−G	134.0(4)	N(2)−Ir−C(17)	91.1(4)
Ir−C(17)−O(1)	177.4(6)	N(2)−Ir−C(18)	168.7(4)
Ir−C(18)−O(2)	178.4(6)	N(4)−Ir−C(17)	166.7(4)
Os−Ir−I	158.71(3)	N(4)−Ir−C(18)	89.2(4)
Os−Ir−C(17)	94.8(3)	C(17)−Ir−C(18)	92.1(5)
Os−Ir−C(18)	97.0(3)		

[a] G represents the centroid of the *p*-cymene ring.

The coordination polyhedron around the iridium atom in **10** is a distorted octahedron, with the two pyrazolate nitrogens and two CO groups in an ideal equatorial plane and the metal−metal bond and the iodide ligand in the relative apical positions. The Os−Ir−I angle of

(27) Pinillos, M. T.; Elduque, A.; Oro, L. A.; Lahoz, F. J.; Bonati, F.; Tiripicchio, A.; Tiripicchio-Camellini, M. *J. Chem. Soc., Dalton Trans.* **1990**, 989.

Table 3. Selected Bond Distances (Å) and Angles (deg) for the Complex [(η^6-*p*-cymene)Os(μ-pz)$_2$RhI(CO)] (12)[a]

Os−Rh	2.6936(9)	Rh−I	2.6724(12)
Os−N(1)	2.070(9)	Rh−I′	2.9368(11)
Os−N(3)	2.058(8)	Rh−N(2)	2.019(8)
Os−C(7)	2.193(12)	Rh−N(4)	2.056(9)
Os−C(8)	2.156(11)	Rh−C(17)	1.851(12)
Os−C(9)	2.198(11)	C(17)−O(1)	1.107(15)
Os−C(10)	2.206(10)	N(1)−N(2)	1.343(11)
Os−C(11)	2.186(9)	N(3)−N(4)	1.362(10)
Os−C(12)	2.192(10)		
Rh−Os−N(1)	69.7(2)	I′-Rh−N(2)	98.5(2)
Rh−Os−N(3)	69.6(2)	I′−Rh−N(4)	91.9(2)
Rh−Os−G[b]	138.5(3)	I′−Rh−C(17)	100.1(3)
N(1)−Os−N(3)	83.5(3)	I′−Rh−I	89.45(3)
N(1)−Os−G	134.6(4)	N(2)−Rh−N(4)	84.8(3)
N(3)−Os−G	133.9(4)	N(2)−Rh−C(17)	94.7(4)
Rh−C(17)−O(1)	177.5(11)	N(2)−Rh−I	170.2(2)
Os−Rh−I	99.04(3)	N(4)−Rh−C(17)	167.9(5)
Os−Rh−I′	162.02(3)	N(4)−Rh−I	89.3(2)
Os−Rh−C(17)	95.8(3)	C(17)−Rh−I	89.4(4)
Rh−I−Rh′	90.55(3)		

[a] Primed atoms are related to the unprimed ones by the symmetry transformation $-x, -y, -z$. [b] G represents the centroid of the *p*-cymene ring.

Table 4. Geometrical Parameters of the Os(μ-pz)$_2$M′ Metallacycles[a]

	6 (M = Rh)	**8** (M = Rh)	**10** (M = Ir)	**12** (M = Rh)
Os−M, Å	3.6231(5)	3.7012(6)	2.7196(6)	2.6936(9)
α, deg	84.05(14)	76.29(16)	52.2(3)	52.3(2)
β, deg	71.37(10)	65.35(11)	89.56(18)	89.7(2)
Q, Å	1.177(2)	1.070(3)	1.584(5)	1.578(5)
Φ, deg	0.56(19)	−3.5(2)	0.4(3)	1.8(3)
θ, deg	86.36(16)	84.3(2)	89.9(2)	90.2(2)

[a] α is the dihedral angle between the coordination planes of the two metals; β is the dihedral angle between the two Os−N−N−M planes; Q, Φ, and θ are the Cremer and Pople parameters.

158.71(3)° reveals the transoid disposition of the halogen and osmium and also explains the very long Ir−I bond distance found[28] (2.8127(10) Å), which is likely to be due to the high *trans* influence of the metal−metal bond.

Complex **12** crystallizes as a dimer of two dinuclear moieties, with two iodine atoms asymmetrically bridging the rhodium centers. As for the iridium in **10,** the coordination polyhedron around the rhodium atom is a distorted octahedron, with ideal equatorial positions occupied by the two pyrazolate nitrogens, the CO group, and one iodide ligand; one apical position is occupied by the Os atom, permitting the iodine atom of another dinuclear moiety to coordinate to the rhodium through the remaining apical position and, consequently, leading to a tetranuclear complex. The two Rh−I bond distances are different; the distance with the iodide ligand *trans* to N(2) is 2.6724(12) Å, while the bond length with the iodine atom in a *trans* disposition to the Os−Rh bond is significantly longer (2.9368(11) Å), as observed in **10**.

Theoretical Studies. The isomerization processes between metal−metal-bonded and unbonded compounds, observed both for RuIr and OsIr complexes, prompted us to carry out a theoretical analysis of the electronic structure of the species involved. It was believed that such a study would shed some light on the energy factors governing these processes and would form the basis for the relative stabilization of the two isomers. We carried out a detailed analysis of the nature of the metal−metal bond in the RuIr complex [(η^6-*p*-cymene)Ru(μ-pz)$_2$IrCl(CO)$_2$] (**13b**) and of the comparative stability of [(η^6-*p*-cymene)RuCl(μ-pz)$_2$Ir(CO)$_2$] (**13a**) and **13b** and their bromide and iodide homologues. This study can be generalized to include the OsIr-containing analogues **5a**,**b**. The calculations were performed by means of extended Hückel molecular orbital calculations using standard programs and atomic parameters.[29]

On a simple electron count basis, the metal−metal bond in **13b** can be formally described as a covalent link between two d^7 centers, Ru(I)−Ir(II), or as a donor−acceptor interaction to d^6 Ru(II) from d^8 Ir(I). The coordination geometry of **13b** agrees with any of these proposals. Metal−metal-bonded species with geometries similar to those found here are known for Ir(II)[19a] and Ru(I),[4c] whereas donor−acceptor metal−metal interactions are also known for Ir(I).[30] On the other hand, the ν(CO) stretching frequencies give information about the electronic density at the metal center. The ν(CO) absorptions observed for complex **13b** (2080, 2020 cm^{-1}) are slightly shifted toward higher frequencies in relation to those found for **13a** (2065, 1995 cm^{-1}). As complex **13a** contains one ruthenium(II) and one iridium(I), this reveals a shift of electron density out of the iridium atom in **13b**, in agreement with a partially oxidized iridium atom, either by a dative Ir(I)−Ru(II) bond or a direct Ir(II)−Ru(I) covalent bond. This behavior has also been observed in the osmium complexes described above: complex **5b** shows two absorptions at 2081 and 2023 cm^{-1} that are shifted to lower wavenumbers in **5a** (2060 and 1996 cm^{-1}).

We have carried out a set of extended Hückel calculations in order to understand the nature of the metal−metal bond in **13b**. When the direct overlap between the two metal atoms is forced to be zero in the calculations to simulate the absence of metal−metal interaction, the seven highest occupied orbitals of the complex show a predominant d character. A Mulliken population analysis indicates that two of these MO's are centered on the ruthenium atom and three on the iridium atom. The remaining two are the result of an equal participation of the two metals. As all of them are doubly

(28) (a) Ciriano, M. A.; Viguri, F.; Oro, L. A.; Tiripicchio, A.; Tiripicchio-Camellini, M. *Angew. Chem., Int. Ed. Engl.* **1987**, *26*, 444. (b) Maverick, A. W.; Smith, T. P.; Maverick, E. F.; Gray, H. B. *Inorg. Chem.* **1987**, *26*, 4336. (c) Ciriano, M. A.; Sebastian, S.; Oro, L. A.; Tiripicchio, A.; Tiripicchio-Camellini, M.; Lahoz, F. J. *Angew. Chem., Int. Ed. Engl.* **1988**, *27*, 402. (d) Vaartstra, B. A.; Xiao, J.; Jenkins, J. A.; Verhagen, R.; Cowie, M. *Organometallics* **1991**, *10*, 2708. (e) Crispini, A.; De Munno, G.; Ghedini, M.; Neve, F. *Inorg. Chem.* **1992**, *31*, 4700. (f) Xiao, J.; Santarsiero, B. D.; Vaartstra, B. A.; Cowie, M. *J. Am. Chem. Soc.* **1993**, *115*, 3212. (g) Xiao, J.; Cowie, M. *Organometallics* **1993**, *12*, 463. (h) Crispini, A.; Ghedini, M.; Neve, F. *Inorg. Chim. Acta* **1993**, *209*, 235. (i) Asseid, F.; Browning, J.; Dixon, K. R.; Meanwell, N. J. *Organometallics* **1994**, *13*, 760. (j) Ciriano, M. A.; Dias, A. R.; Nunes, P. M.; Oro, L. A.; Minas da Piedade, M. F.; Minas da Piedade, M. E.; Ferreira da Silva, P.; Martinho Simoes, J. A.; Pérez-Torrente, J. J.; Veiros, L. F. *Struct. Chem.* **1996**, *7*, 337. (k) Kuang, S. M.; Xue, F.; Zhang, Z.-Z.; Xue, W.-M.; Che, C.-M.; Mak, T. C. W. *J. Chem. Soc., Dalton Trans.* **1997**, 3409. (l) Tejel, C.; Ciriano, M. A.; López, J. A.; Lahoz, F. J.; Oro, L. A. *Angew. Chem., Int., Ed. Engl.* **1998**, *37*, 1542.

(29) (a) Hoffmann, R. *J. Chem. Phys.* **1963**, *39*, 1397. (b) Hoffmann, R.; Lipscomb, W. N. *J. Chem. Phys.* **1962**, *36*, 2179, 2872. (c) Howell, J.; Rossi, A.; Wallace, D.; Haraki, K.; Hoffmann, R. *QCPE* **1977**, *11*, 344.

(30) (a) Oro, L. A.; Sola, E.; López, J. A.; Torres, F.; Elduque, A.; Lahoz, F. J. *Inorg. Chem. Commun.* **1998**, *1*, 64. (b) Tejel, C.; Ciriano, M. A.; López, J. A.; Lahoz, F. J.; Oro, L. A. *Organometallics* **1997**, *16*, 4718.

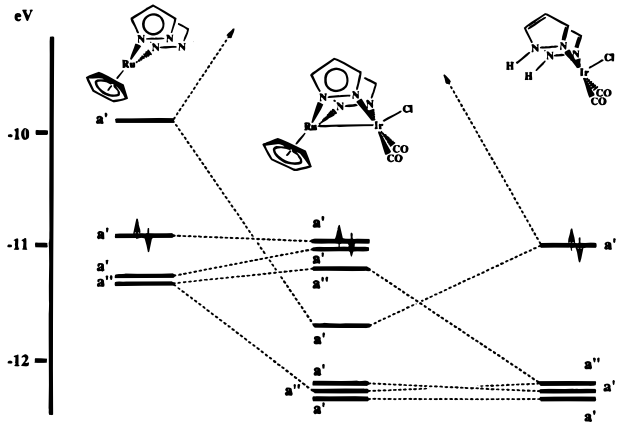

Figure 5. MO diagram showing the relationship between the molecular orbitals of the pseudofragments [IrCl(CO)$_2$(Hpz)$_2$] and [Ru(pz)$_2$(η^6-C$_6$H$_6$)] and the electronic structure of **13b**.

occupied the electron count would be equivalent to a formal d^8 electron configuration for the iridium atom and a d^6 configuration for the ruthenium center. Furthermore, these frontier orbitals, in which the lack of direct metal−metal interaction has been simulated, can be matched to the superposition of the molecular orbitals of the two hypothetical independent complexes [IrCl(CO)$_2$(Hpz)$_2$] and [Ru(pz)$_2$(η^6-C$_6$H$_6$)]. When the intermetallic overlap is switched on, the interaction between the metal atoms can be described as a donor−acceptor bond between the HOMO of the pentacoordinated pseudofragment [IrCl(CO)$_2$(Hpz)$_2$] and the LUMO of [Ru(pz)$_2$(η^6-C$_6$H$_6$)] (Figure 5). The rest of the orbitals, which have a significant d character, remain basically unaltered and have a nonbonding role with respect to the metal−metal interaction. Although this simple theoretical model seems to support the idea of a donor−acceptor bond between d^8 Ir(I) and d^6 Ru(II), which implies a partial oxidation of the iridium in **13b** (as indicated by the IR measurements), the possibility of a covalent bond between two different d^7 centers (Ir(II)−Ru(I)) cannot be excluded, both theoretically and chemically. The latter view would suggest that the chlorotropic shift leads to a redox tautomerism between species **13a** and **13b** (Ir(I)−Ru(II) and Ir(II)−Ru(I)) similar to that recently observed for the diiridium complexes [(CNBu^t)$_2$Ir(μ-pz)$_2$Ir(Cl)(CH$_2$Ph)(CNBu^t)$_2$] and [(CNBu^t)$_2$(Cl)Ir(μ-pz)$_2$Ir(CH$_2$Ph)(CNBu^t)$_2$][31] (Ir(I)−Ir(III) and Ir(II)−Ir(II)).

The relative stability of the isomers **13a** and **13b** was studied by a fragment analysis of the interaction of a chloride anion with the cationic fragments **13a**$^+$ and **13b**$^+$. The studies of both isomers showed a slightly higher stability for **13a** than for **13b**, a trend in accord with previous experimental equilibrium data. Nevertheless, the most stable cationic fragment is **13b**$^+$, rather than **13a**$^+$, indicating that the origin of the difference in stability is the distinct interaction with the chloride ligand. Thus, in both complexes (**13a** and **13b**) the interaction between the chloride ligand and the metal atoms leads to the bonding−antibonding linear combinations that give rise to a stabilization of the atomic orbitals of the chlorine atom. This is because they play

(31) Tejel, C.; Ciriano, M. A.; López, J. A.; Lahoz, F. J.; Oro, L. A. *Organometallics* **1998**, *17*, 1449.

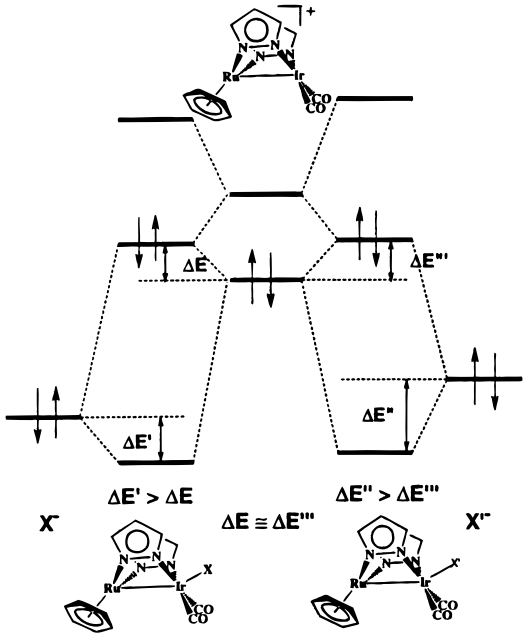

Figure 6. Schematic interaction diagram between two different halide ions, X$^-$ and X′$^-$, with the fragment **13b**$^+$.

a predominant role in the bonding combinations and there is a major contribution of the metal orbitals in the corresponding antibonding linear combinations. In complex **13a** the interaction between the chloride ligand an the ruthenium atom is of a donor−acceptor type and the antibonding orbitals remain unoccupied. On the other hand, in complex **13b** the interaction takes place essentially between the chloride ligand and the occupied d orbitals of the iridium atom, which generates a typical nonstabilizing two-orbital−four-electron combination (Figure 6). This situation would not be stable at all in the absence of additional effects created by the mixing with other orbitals. In fact, the admixture of the LUMO of the pseudofragment [Ru(pz)$_2$(η^6-C$_6$H$_6$)] into the antibonding Ir−Cl orbital has a bonding character relative to the metal−metal interaction, and this can be traced as the origin of the metal−metal bond of order 1. This admixture counteracts the destabilizing effect of this antibonding orbital and means a transfer of electronic density from the halogen to the ruthenium atom through the iridium center and the metal−metal bond.

The electronegativity of the halogen ligand decreases when the chloride ligand is replaced by bromide or iodide, and there is a better match in the energies of the occupied orbitals on iridium and those of the orbitals of the halogen atom. As expected, the more favorable interaction has a stabilizing effect in the bonding linear combinations but also should have a greater increase in energy in the antibonding ones. Indeed, the calculations show a progressive stabilization of the bonding linear combination, but its antibonding counterpart hardly changes in energy. This is due to the mixing with the LUMO of the ruthenium-containing moiety. The global energy balance of this interaction makes the metal−metal-bonded isomer more stable on changing from chlorine to iodine, as the more favorable bonding interaction is not canceled by its antibonding occupied counterpart, which in fact remains at an almost constant energy value in all the halogen complexes. The replacement of Ru for Os has a similar effect, in this

case owing to the more favorable metal−metal interaction in the OsIr species, which is reflected in the increased stability for the metal−metal-bonded isomers.

Experimental Section

General Comments. All reactions were carried out using standard Schlenk techniques. All solvents were dried, distilled under N_2, and degassed prior to use. Infrared spectra were recorded on Perkin-Elmer 783 and 1330 spectrophotometers (range 4000−200 cm^{-1}) using Nujol mulls between polyethylene sheets or dichloromethane solutions between NaCl plates. ^1H and ^{13}C NMR spectra were recorded on a Varian XL-300 spectrometer (300.0 (^1H) or 75.4 (^{13}C) MHz). The chemical shifts were measured relative to partially deuterated solvent peaks but are reported in parts per million (ppm) relative to tetramethylsilane. Mass spectra were measured on a VG Autospec double-focusing mass spectrometer operating in the FAB^+ mode. Ions were produced with the standard Cs^+ gun at ca. 30 kV, and 3-nitrobenzyl alcohol (NBA) was used as a matrix. The C, H, and N analyses were carried out with a Perkin-Elmer 240B microanalyzer.

Preparation of [(η^6-*p*-cymene)OsCl(Hpz)$_2$]Cl (1). To a suspension of [{(η^6-*p*-cymene)OsCl}$_2$(μ-Cl)$_2$] (0.102 g, 0.13 mmol) in MeOH (5 mL) was added Hpz (0.037 g, 0.54 mmol). After the mixture was stirred for 30 min, the resulting solution was concentrated under reduced pressure. The slow addition of diethyl ether led to the precipitation of a yellow solid, which was filtered off, washed with diethyl ether, and air-dried. Yield: 77%. Anal. Calcd for $C_{16}H_{22}Cl_2N_4Os$: C, 36.2; H, 4.1; N, 10.5. Found: C, 36.4; H, 4.15; N, 10.8. IR (Nujol mull): ν(NH) 3321 (s), 3200−2500 (m) cm^{-1}. ^1H NMR ($CDCl_3$, δ): 14.45 (bs, 2H, NH); 8.01 (dt, 2H, $^3J(H_4H_3) = 2.1$, $^4J(H_1H_3) = 2.1$, $^4J(H_5H_3) = 0.7$ Hz, H_3 of Hpz); 7.64 (ddd, 2H, $^3J(H_4H_5) = 2.2$, $^3J(H_1H_5) = 1.8$ Hz, H_5 of Hpz); 6.23 (q, 2H, $^4J(H_1H_4) = 2.1$ Hz, H_4 of Hpz); 6.15, 6.19 (AA′BB′ system, J(AB) = J(A′B′) = 5.8 Hz, C_6H_4); 2.04 (sp, 1H, C*H*Me$_2$); 1.75 (s, 3H, Me); 1.03 (d, 6H, ^3J(HH) = 6.9 Hz, CH*Me*$_2$). MS (FAB^+): *m*/*z* 361 (M^+ − 2Hpz, 20%); 393 (M^+ − Cl − Hpz, 9%); 429 (M^+ − Hpz, 100%); 497 (M^+, 49%).

Preparation of [(η^6-*p*-cymene)OsCl(Hpz)$_2$]BF$_4$ (2). Hpz (0.256 g, 3.69 mmol) and $NaBF_4$ (93%) (0.224 g, 1.89 mmol) were added to a suspension of [{(η^6-*p*-cymene)OsCl}$_2$(μ-Cl)$_2$] (0.728 g, 0.92 mmol) in methanol (15 mL). The suspension was stirred for 2 h and then evaporated to dryness. The residue was extracted with dichloromethane (3 × 20 mL) and the resulting solution concentrated to ca. 2 mL. The slow addition of diethyl ether led to the precipitation of a yellow solid, which was filtered off, washed with diethyl ether, and air-dried. Yield: 87%. Anal. Calcd for $C_{16}H_{22}ClN_4BF_4Os$: C, 33.0; H, 3.8; N, 9.6. Found: C, 32.75; H, 3.9; N, 9.5. IR (Nujol mull): ν(NH) 3321 (vs), 3200−2500 (m) cm^{-1}. ^1H NMR ($CDCl_3$, δ): 12.05 (bs, 2H, NH); 8.12 (dd, 2H, $^3J(H_4H_3) = 2.3$, $^4J(H_5H_3) = 0.6$ Hz, H_3 of Hpz); 7.56 (dd, 2H, $^3J(H_4H_5) = 2.8$ Hz, H_5 of Hpz); 6.36 (t, 2H, H_4 of Hpz); 6.07, 6.17 (AA′BB′ system, J(AB) = J(A′B′) = 5.8 Hz, C_6H_4); 2.32 (sp, 1H, C*H*Me$_2$); 1.86 (s, 3H, Me); 1.07 (d, 6H, ^3J(HH) = 7.0 Hz, CH*Me*$_2$).

Preparation of [(η^6-*p*-cymene)OsCl(μ-pz)$_2$Ir(COD)] (3). To a solution of [(η^6-*p*-cymene)OsCl(Hpz)$_2$]BF_4 (0.198 g, 0.34 mmol) in acetone (30 mL), under nitrogen, was added [Ir(μ-OMe)(COD)]$_2$ (0.113 g, 0.17 mmol) and KOH in MeOH (1.2 mL, 0.2800 N, 0.34 mmol). After the mixture was stirred for 15 min, the resulting suspension was extracted with dichloromethane (6 × 15 mL) and the solution concentrated under reduced pressure to ca. 2 mL. The slow addition of *n*-hexane led to the precipitation of an orange precipitate, which was filtered off, washed with *n*-hexane, and air-dried. Yield: 62%. Anal. Calcd for $C_{24}H_{32}ClN_4OsIr$: C, 36.3; H, 4.0; N, 7.05. Found: C, 36.3; H, 3.9; N, 7.0. ^1H NMR ($CDCl_3$, δ): 7.63 (d, 2H, $H_{3/5}$ of pz); 7.34 (d, 2H, $H_{5/3}$ of pz); 6.05 (t, 2H, $^3J(H_3H_4) = {}^3J(H_5H_4) = 1.7$ Hz, H_4 of pz); 6.01, 6.09 (AA′BB′ system, J(AB) = J(A′B′) = 5.4 Hz, C_6H_4); 4.01 (m, 2H, vinylic CH); 3.56 (m, 2H, vinylic CH); 2.38 m (5H, CH_2 of COD and C*H*Me$_2$ of *p*-cymene); 1.77 (s, 3H, Me); 1.68 (m, 4H, CH_2); 1.15 (d, 6H, ^3J(HH) = 6.8 Hz, CH*Me*$_2$).

[(η^6-*p*-cymene)OsCl(μ-pz)$_2$Rh(COD] (**4**) was prepared in a way similar to that given above. The reaction time was 23 h. Yield: 89%. Anal. Calcd for $C_{24}H_{32}ClN_4OsRh$: C, 40.9; H, 4.5; N, 7.9. Found: C, 41.15; H, 4.7; N, 7.8. ^1H NMR ($CDCl_3$, δ): 7.59 (d, 2H, $H_{3/5}$ of pz); 7.20 (d, 2H, $H_{5/3}$ of pz); 5.98 (t, 2H, $^3J(H_3H_4) = {}^3J(H_5H_4) = 2.1$ Hz, H_4 of pz); 6.11, 6.28 (AA′BB′ system, J(AB) = J(A′B′) = 5.2 Hz, C_6H_4); 4.34 (m, 2H, CH of COD); 3.90 m (2H, CH of COD); 2.56 (m, 4H, CH_2); 2.38 (sp, 1H, C*H*Me$_2$); 1.91 (m, 4H, CH_2); 1.78 (s, 3H, Me); 1.17 (d, 6H, ^3J(HH) = 6.9 Hz, CH*Me*$_2$).

Preparation of [(η^6-*p*-cymene)OsCl(μ-pz)$_2$Ir(CO)$_2$] (5a). Bubbling of carbon monoxide (atmospheric pressure, room temperature) for 3 h through a CH_2Cl_2 (30 mL) solution of compound **3** (0.238 g, 0.30 mmol) led to an orange solution, which was partially concentrated under reduced pressure. The slow addition of *n*-hexane gave complex **5a** as a brown solid, which was filtered off, washed with *n*-hexane, and air-dried. The complex was recrystallized from diethyl ether/hexane. Yield: 82%. Anal. Calcd for $C_{18}H_{20}ClN_4O_2OsIr$: C, 29.1; H, 2.7; N, 7.55. Found: C, 29.5; H, 2.2; N, 7.5. IR (CH_2Cl_2): ν(CO) 2068 (vs), 1996 (vs) cm^{-1}. ^1H NMR ($CDCl_3$, δ): 7.64 (dd, 2H, $^4J(H_5H_3) = 0.7$ Hz, $H_{3/5}$ of pz); 7.45 (dd, 2H, $H_{5/3}$ of pz); 6.16 (t, 2H, $^3J(H_3H_4) = {}^3J(H_5H_4) = 2.3$ Hz, H_4 of pz); 5.88, 5.91 (AA′BB′ system, J(AB) = J(A′B′) = 5.9 Hz, C_6H_4); 2.47 (sp, 1H, C*H*Me$_2$); 1.79 (s, 3H, Me); 1.16 (d, 6H, ^3J(HH) = 6.9 Hz, CH*Me*$_2$).

Complex **6** was prepared in a way similar to that given above. Yield: 85%. Anal. Calcd for $C_{18}H_{20}ClN_4O_2OsRh$: C, 33.1; H, 3.1; N, 8.6. Found: C, 33.1; H, 3.8; N, 8.25. IR (CH_2Cl_2): ν(CO) 2081 (vs), 2014 (vs) cm^{-1}. ^1H NMR ($CDCl_3$, δ): 7.63 (d, 2H, $H_{3/5}$ of pz); 7.33 (d, 2H, $H_{5/3}$ of pz); 6.12 (t, 2H, $^3J(H_3H_4) = {}^3J(H_5H_4) = 2.1$ Hz, H_4 of pz); 5.90 (bs, 4H, C_6H_4); 2.46 (sp, 1H, C*H*Me$_2$); 1.76 (s, 3H, Me); 1.15 (d, 6H, ^3J(HH) = 6.9 Hz, CH*Me*$_2$). $^{13}C\{^1H\}$ NMR ($CDCl_3$, δ): 185.8 (d, ^1J(CRh) = 65.6 Hz, CO); 142.9 (s, $C_{3/5}$ of pz), 140.6 (s, $C_{5/3}$ of pz); 105.7 (s, C_4 of pz); 92.6 (s,*C*Me of *p*-cymene); 93.6 (s, *C*CHMe$_2$ of *p*-cymene); 78.0 (s, $C_{AA'/BB'}$, of *p*-cymene); 73.1 (s, $C_{BB'/AA'}$ of *p*-cymene); 31.0 (s, *C*HMe$_2$); 22.8 (s, CH*Me*$_2$); 17.8 (s, Me). MS (FAB^+): *m*/*z* 493 (M^+ − Cl − pz − 2CO, 84%); 559 (M^+ − Cl − 2CO, 52%); 598 (M^+ − 2CO, 84%); 619 (M^+ − Cl, 100%); 654 (M^+, 24%).

Preparation of [(η^6-*p*-cymene)Os(μ-pz)$_2$IrCl(CO)$_2$] (5b). A suspension of [(η^6-*p*-cymene)OsCl(μ-pz)$_2$Ir(CO)$_2$] (**5a**) in MeOH (5 mL) was stirred for 24 h. The precipitate that formed was filtered off, washed with methanol, and air-dried. Yield: 70%. Anal. Calcd for $C_{18}H_{20}ClN_4O_2OsIr$: C, 29.1; H, 2.7; N, 7.55. Found: C, 28.8; H, 2.8; N, 7.3. IR (CH_2Cl_2): ν(CO) 2081 (vs), 2023 (vs) cm^{-1}. ^1H NMR ($CDCl_3$, δ): 7.59 (d, 2H, $H_{3/5}$ of pz); 7.35 (d, 2H, $H_{5/3}$ of pz); 5.93 (t, 2H, $^3J(H_3H_4) = {}^3J(H_5H_4) = 2.2$ Hz, H_4 of pz); 5.64, 5.77 (AA′BB′ system, J(AB) = J(A′B′) = 5.4 Hz, C_6H_4); 2.54 (sp, 1H, C*H*Me$_2$); 2.21 (s, 3H, Me); 1.08 (d, 6H, ^3J(HH) = 6.9 Hz, CH*Me*$_2$).

Preparation of [(η^6-*p*-cymene)Os(CO)(μ-pz)$_2$Ir(CO)$_2$]-BPh$_4$ (7). Bubbling of carbon monoxide (atmospheric pressure, room temperature) for 2 h through a solution of [(η^6-*p*-cymene)-OsCl(μ-pz)$_2$Ir(COD)] (**3**; 0.101 g, 0.13 mmol) and $NaBPh_4$ (0.053 g, 0.15 mmol) in methanol (30 mL) led to the precipitation of a yellow solid, which was filtered off, washed with methanol, and air-dried. Yield: 44%. Anal. Calcd for $C_{43}H_{40}BN_4O_3OsIr$: C, 49.0; H, 3.8; N, 5.3. Found: C, 48.6; H, 4.3; N, 5.2. IR (CH_2Cl_2): ν(CO) 2079 (vs), 2012 (br) cm^{-1}. ^1H NMR (CD_2Cl_2, δ): 7.57 (d, 2H, $H_{3/5}$ of pz); 7.5−6.8 (bm, 22H, $H_{5/3}$ of pz and 4Ph); 6.35 (t, 2H, $^3J(H_3H_4) = {}^3J(H_5H_4) = 2.4$ Hz, H_4 of pz); 5.74 (s, 4H, C_6H_4); 2.46 (sp, 1H, C*H*Me$_2$); 1.67 (s, 3H, Me); 1.12 (d, 6H, ^3J(HH) = 6.9 Hz, CH*Me*$_2$). MS (FAB^+): *m*/*z* 649 (M^+ − 3CO, 26%); 677 (M^+ − 2CO, 46%); 707 (M^+ − CO, 100%); 735 (M^+, 69%).

Table 5. Crystallographic Data and Refinement Details for 6, 8, 10, and 12

	6	8	10	12
cryst color, habit	yellow, irregular block	orange, prismatic block	reddish, irregular block	orange, prismatic block
cryst size, mm	0.52 × 0.42 × 0.36	0.36 × 0.18 × 0.08	0.17 × 0.15 × 0.10	0.26 × 0.20 × 0.14
chem formula	$C_{18}H_{20}ClN_4O_2OsRh$	$C_{43}H_{40}BN_4O_3OsRh$	$C_{18}H_{20}IIrN_4O_2Os$	$C_{17}H_{20}IN_4OOsRh$
fw	652.94	964.71	833.68	716.38
cryst syst	monoclinic	triclinic	orthorhombic	monoclinic
space group	$P2_1/n$ (No. 14)	$P\bar{1}$ (No. 2)	$P2_12_12_1$ (No. 19)	$P2_1/c$ (No. 14)
a, Å	11.9551(11)	9.7378(8)	9.5321(11)	9.2213(15)
b, Å	14.0018(13)	11.2371(11)	12.7061(15)	13.577(2)
c, Å	12.4844(12)	18.8008(14)	17.9660(13)	16.009(2)
α, deg	90	73.716(6)	90	90
β, deg	99.183(8)	83.814(6)	90	102.544(12)
γ, deg	90	78.431(7)	90	90
V, Å³	2063.0(4)	1931.7(3)	2176.0(4)	1956.5(5)
Z	4	2	4	4
ρ(calcd), g cm^{-3}	2.102	1.659	2.545	2.432
μ, mm^{-1}	7.102	3.757	13.381	8.922
θ range data collecn, deg	2.19−35.02	1.92−27.50	1.96−24.98	1.99−25.02
index ranges	$-1 \le h \le 14$, $-1 \le k \le 22$, $-20 \le l \le 20$	$-1 \le h \le 12$, $-13 \le k \le 14$, $-24 \le l \le 24$	$-11 \le h \le 1$, $-15 \le k \le 0$, $-21 \le l \le 21$	$-5 \le h \le 10$, $0 \le k \le 16$, $-19 \le l \le 9$
no. of unique rflns	5959 (R_{int} = 0.0465)	6328 (R_{int} = 0.0632)	3832 (R_{int} = 0.0265)	3438 (R_{int} = 0.0582)
min, max transmissn factors	0.022, 0.068	0.377, 0.533	0.458, 1.000[d]	0.035, 0.062
no. of data/ restraints/params	5959/0/250	6328/0/485	3832/75/250	3438/30/232
$R(F)$ ($F^2 > 2\sigma(F^2)$)[a]	0.0314	0.0365	0.0321	0.0425
$R_w(F^2)$ (all data)[b]	0.0753	0.0769	0.0498	0.0675
S (all data)[c]	0.937	0.900	1.015	0.973

[a] $R(F) = \sum||F_o| - |F_c||/\sum|F_o|$ for 4607, 6328, 3263, and 2381 observed reflections, respectively. [b] $R_w(F^2) = [\sum[w(F_o^2 - F_c^2)^2]/\sum[w(F_o^2)^2]]^{1/2}$; $w^{-1} = [\sigma^2(F_o^2) + (aP)^2]$, where $P = [\max(F_o^2, 0) + 2F_c^2]/3$ (**6**:, $a = 0.0454$; **8**, $a = 0.0369$; **10**, $a = 0.0160$; **12**, $a = 0.0151$). [c] $S = [\sum[w(F_o^2 - F_c^2)^2]/(n - p)]^{1/2}$, where *n* is the number of reflections and *p* the number of parameters. [d] Correction factors are included.

Preparation of [(η⁶-*p*-cymene)Os(CO)(μ-pz)₂Rh(CO)₂]-BPh₄ (8). Bubbling of carbon monoxide (atmospheric pressure, room temperature) for 3 h through a suspension of [(η⁶-*p*-cymene)-OsCl(μ-pz)₂Rh(COD)] (**4**; 0.101 g, 0.14 mmol) in methanol (25 mL) gave a yellow solution. The addition of $NaBPh_4$ (0.059 g, 0.17 mmol) led to the precipitation of a yellow solid, which was filtered off, washed with methanol, and air-dried. Yield: 64%. Anal. Calcd for $C_{43}H_{40}BN_4O_3OsRh$: C, 53.55; H, 4.15; N, 5.8. Found: C, 53.3; H, 4.05; N, 5.6. IR (CH_2Cl_2): *ν*(CO) 2093 (vs), 2029 (br) cm^{-1}. ^{1}H NMR (CD_2Cl_2, *δ*): 7.45 (d, 2H, $H_{3/5}$ of pz); 7.4−6.8 (bm, 22H, $H_{5/3}$ of pz and 4Ph); 6.30 (t, 2H, $^3J(H_3H_4) = {}^3J(H_5H_4) = 2.4$ Hz, H_4 of pz); 5.76 (s, 4H, C_6H_4); 2.45 (sp, 1H, C*H*Me₂); 1.66 (s, 3H, Me); 1.12 (d, 6H, ^3J(HH) = 6.9 Hz, CH*Me*₂). MS (FAB$^+$): *m*/*z* 561 (M$^+$ − 3CO, 13%); 619 (M$^+$ − CO, 29%); 647 (M$^+$, 100%).

Complex **8** can be also prepared starting from [(η⁶-*p*-cymene)OsCl(μ-pz)₂Rh(CO)₂] (**6**) using the method described above. Yield: 65%.

Preparation of [(η⁶-*p*-cymene)Os(μ-pz)₂IrI(CO)₂] (10). Under nitrogen, to a solution of [(η⁶-*p*-cymene)OsCl(μ-pz)₂Ir-(CO)₂] (0.102 g, 0.14 mmol) in methanol (15 mL) was added NaI·2H₂O (0.403 g, 2.17 mmol). The solution was stirred for 2 h and then evaporated to dryness. The residue was extracted with dichloromethane (3 × 10 mL) and the extract evaporated to ca. 2 mL. The slow addition of *n*-hexane led to the precipitation of an orange solid, which was filtered off, washed with *n*-hexane, and air-dried. Yield: 57%. Anal. Calcd for $C_{18}H_{20}IIrN_4O_2Os$: C, 25.9; H, 2.4; N, 6.7. Found: C, 26.4; H, 2.0; N, 6.7. IR (CH_2Cl_2): *ν*(CO) 2025 (vs), 2079 (vs) cm^{-1}. ^{1}H NMR ($CDCl_3$, *δ*): 7.59 (d, 2H, $H_{3/5}$ of pz); 7.36 (d, 2H, $H_{5/3}$ of pz); 5.88 (t, 2H, $^3J(H_3H_4) = {}^3J(H_5H_4) = 2.2$ Hz, H_4 of pz); 5.67, 5.80 (AA′BB′ system, $J(AB) = J(A'B') = 5.6$ Hz, C_6H_4); 2.54 (sp, 1H, C*H*Me₂); 2.22 (s, 3H, Me); 1.08 (d, 6H, ^3J(HH) = 6.9 Hz, CH*Me*₂). MS (FAB$^+$): *m*/*z* 677 (M$^+$ − I − CO, 13%); 707 (M$^+$ − I, 100%); 806 (M$^+$ − CO, 10%); 833 (M$^+$, 11%).

[(η⁶-*p*-cymene)Os(μ-pz)₂IrBr(CO)₂] (**9**) and [(η⁶-*p*-cymene)-OsBr(μ-pz)₂Rh(CO)₂] (**11**) were prepared in a way similar to that given above, but with sodium bromide.

Complex 9. Yield: 66%. Anal. Calcd for $C_{18}H_{20}BrIrN_4O_2$-Os: C, 27.5; H, 2.5; N,7.1. Found: C, 28.1; H, 2.15; N, 7.1. IR (CH_2Cl_2): *ν*(CO) 2025 (vs), 2081 (vs) cm^{-1}. ^{1}H NMR ($CDCl_3$, *δ*): 7.59 (d, 2H, $H_{3/5}$ of pz); 7.35 (d, 2H, $H_{5/3}$ of pz); 5.91 (t, 2H, $^3J(H_3H_4) = {}^3J(H_5H_4) = 2.1$ Hz, H_4 of pz); 5.66, 5.79 (AA′BB′ system, $J(AB) = J(A'B') = 5.2$ Hz, C_6H_4); 2.54 (sp, 1H, C*H*Me₂); 2.22 (s, 3H, Me); 1.07 (d, 6H, ^3J(HH) = 6.9 Hz, CH*Me*₂). MS (FAB$^+$): *m*/*z* 707 (M$^+$ − Br, 100%); 733 (M$^+$ − 2CO, 20%); 760 (M$^+$ − CO, 36%); 788 (M$^+$, 33%).

Complex 11. Yield: 65%. Anal. Calcd for $C_{18}H_{20}BrN_4O_2$-OsRh: C, 31.0; H, 2.9; N, 8.0. Found: C, 30.8; H, 3.05; N, 7.9. IR (CH_2Cl_2): *ν*(CO) 2014, 2081 (vs) cm^{-1}. ^{1}H NMR ($CDCl_3$, *δ*): 7.77 (d, 2H, $H_{3/5}$ of pz); 7.33 (d, 2H, $H_{5/3}$ of pz); 6.11 (t, 2H, $^3J(H_3H_4) = {}^3J(H_5H_4) = 2.2$ Hz, H_4 of pz); 5.96 (s, 4H, C_6H_4); 2.44 (sp, 1H, C*H*Me₂); 1.73 (s, 3H, Me); 1.15 (d, 6H, ^3J(HH) = 6.9 Hz, CH*Me*₂). MS (FAB$^+$): *m*/*z* = 561 (M$^+$ − Br − 2CO, 37%); 619 (M$^+$ − Br, 100%); 670 (M$^+$ − CO, 50%); 698 (M$^+$, 24%).

Preparation of [(η⁶-*p*-cymene)Os(μ-pz)₂RhI(CO)] (12). To a suspension of [(η⁶-*p*-cymene)OsCl(μ-pz)₂Rh(CO)₂] (0.101 g, 0.15 mmol) in methanol (10 mL), under nitrogen, was added NaI·2H₂O (0.154 g, 0.83 mmol). The resulting solution was heated under reflux for 2 h. The orange precipitate that formed was filtered off, washed with methanol, and air-dried. Yield: 67%. Anal. Calcd for $C_{17}H_{20}IN_4OOsRh$: C, 28.5; H, 2.8; N, 7.8. Found: C, 28.3; H, 2.4; N, 7.8. IR (CH_2Cl_2): *ν*(CO) 2017 (vs) cm^{-1}. ^{1}H NMR ($CDCl_3$, *δ*): 7.80 (d, 1H, $H_{3/5}$ of pz); 7.65 (d, 1H, $H_{3/5}$ of pz); 7.48 (d, 1H, $H_{5/3}$ of pz); 7.12 (d, 1H, $H_{5/3}$ of pz); 6.16 (t, 1H, $^3J(H_3H_4) = {}^3J(H_5H_4) = 2.0$ Hz, H_4 of pz); 6.10 (bm, overlapping of the signals of two AB systems, 4H, C_6H_4); 5.96 (t, 1H, $^3J(H_3H_4) = {}^3J(H_5H_4) = 2.0$ Hz, H_4 of pz); 2.63 (sp, 1H, C*H*Me₂); 2.22 (s, 3H, Me); 1.20 (d, 3H, ^3J(HH) = 6.9 Hz, CH*Me*₂); 0.97 (d, 3H, ^3J(HH) = 6.9 Hz, CH*Me*₂).

Crystal X-ray Measurements and Structure Determination of [(η⁶-*p*-cymene)OsCl(μ-pz)₂Rh(CO)₂] (6), [(η⁶-*p*-cymene)Os(CO)(μ-pz)₂Rh(CO)₂]BPh₄ (8), [(η⁶-*p*-cymene)-Os(μ-pz)₂IrI(CO)₂] (10), and [(η⁶-*p*-cymene)Os(μ-pz)₂RhI-

(CO)] (12). Crystals suitable for X-ray diffraction were grown by slow evaporation of a solution of **8** in CH_2Cl_2 or by slow diffusion of pentane into a solution of **6** in Et_2O and of hexane into solutions of **10** in CH_2Cl_2 and **12** in $CHCl_3$. Crystals were glued to the end of glass fibers and mounted on a four-circle diffractometer (Siemens P4 for **6** and **8**, Siemens-Stoe AED-2 for **10** and **12**), working with graphite-monochomated Mo Kα radiation and operating at 200 K. A summary of crystal data, intensity collection procedures, and refinement parameters for the four structural analyses is reported in Table 5. Precise lattice parameters were determined by least-squares fits from 72 (**6**), 56 (**10**), and 47 (**12**) centered reflections in the region $25 \leq 2\theta \leq 38°$ and from 50 reflections in the region $20 \leq 2\theta \leq 35°$ (**8**). Three standard reflections were monitored every 97 measured reflections (**6**, **8**) or every 55 min of measuring time (**10**, **12**) to check crystal and instrument stability throughout data collection; no significant variations of the intensities were observed. All data were corrected for Lorentz and polarization effects, and a semiempirical absorption correction was also applied (ψ-scan method[32] for **6**, **8**, and **12** and ΔF method[33] for **10**); minimum and maximum transmission factors are listed in Table 5. The structures were solved by Patterson and conventional Fourier techniques and refined by full-matrix least-squares methods on F^2 (SHELXL-97)[34] with initial isotropic thermal parameters. Anisotropic thermal parameters were used in the last cycles of refinement for all non-hydrogen atoms. Hydrogen atoms for methyl groups were include in calculated positions (C−H = 0.96 Å), and the remaining hydrogens were located in difference Fourier maps; all were included in the refinement riding on their respective carbon atom with different common isotropic thermal parameters for the distinct types of H atoms. Atomic scattering factors, corrected for anomalous dispersion for heavy atoms, were taken from ref 35.

Acknowledgment. We thank the Dirección General de Investigación Científica y Técnica for financial support (Projects PB96/0845 and PB95/1186). S.E. thanks the DGICYT for a fellowship.

Supporting Information Available: Full listings of crystallographic data, atomic coordinates, isotropic and anisotropic thermal parameters, and bond distances and angles, in CIF format, for complexes **6**, **8**, **10**, and **12**. This material is available free of charge via the Internet at http://pubs.acs.org.

OM990624H

(32) North, A. C. T.; Phillips, D. C.; Mathews, F. S. *Acta Crystallogr., Sect. A* **1968**, *24*, 351.
(33) Walker, N.; Stuart, D. *Acta Crystallogr., Sect. A* **1983**, *39*, 158.
(34) Sheldrick, G. M. SHELXL-97 Program for Crystal Structure Refinement; University of Göttingen, Göttingen, Germany, 1997.
(35) *International Tables For Crystallography*; Kynoch Press: Birmingham, England, 1974; Vol. IV.